Pressure correction for laminar combustion simulation

EINDHOVEN UNIVERSITY OF TECHNOLOGY
Department of Mathematics and Computing Science

RANA 99-05
January 1999

Pressure Correction for Laminar Combustion Simulation

by

B. van 't Hof, J.H.M. ten Thije Boonkkamp,
R.M.M. Mattheij

Reports on Applied and Numerical Analysis
Department of Mathematics and Computing Science
Eindhoven University of Technology
P.O. Box 513
5600 MB Eindhoven, The Netherlands
ISSN: 0926-4507

Pressure Correction for Laminar Combustion Simulation

B. van 't Hof, J.H.M. ten Thije Boonkkamp, R.M.M. Mattheij

Eindhoven University of Technology
Department of Mathematics and Computing Science
P.O. Box 513, 5600 MB Eindhoven, The Netherlands

Abstract

The space discretized conservation equations for laminar flames are formulated as a system of differential algebraic equations (DAEs). An appropriate constraint is derived, which is used in two new pressure correction schemes. Application to flame simulations with a one-step chemistry model shows that these new pressure correction schemes yield more accurate results than the standard scheme.

Key words. pressure correction, differential algebraic equations, constraint equation, laminar flames.

1 Introduction

Simulation of laminar combustion requires very much computer power. The equations are so stiff that only implicit time integration methods, like the Euler Backward scheme, can provide reliable results. Such schemes, however, require the solution of a system which is very difficult to solve. Some of these difficulties arise from the (almost) isobaric conditions at which the laminar combustion process takes place. Traditional pressure correction methods, which have been developed to deal with these difficulties, are not suited to handle combustion. This paper aims to explain the difficulties arising in computing the time steps in the Euler Backward scheme, as well as the unreliable behavior of the standard pressure correction scheme. Consequently, a remedy is proposed and tested on a simple combustion problem.

Pressure correction methods have been applied successfully for the simulation of the incompressible Navier-Stokes equations. These methods may be understood as a projection methods, where a predictor time step is followed by a corrector step, in which the velocity field is adjusted to satisfy the divergence free constraint, as required by the continuity equation.

These pressure correction schemes have also been applied to other equations than the incompressible Navier-Stokes equations [1, 6]. In the current paper, we describe the generalization to laminar combustion problems. Laminar combustion usually occurs at very low convective velocities. Hence the Mach numbers found in laminar flames are often so small that the isobaric, or 'combustion' approximation may be applied. We will show that straightforward application of the pressure correction method as developed for the incompressible Navier-Stokes equations is not suitable, as the continuity equation can no longer be understood as a constraint. After reformulation, the pressure correction methods can be applied successfully. The formulation we derive is known as the 'semi-explicit formulation' in differential algebraic theory [12], where the time derivatives of some unknowns are given explicitly, and the rest of the system is given in terms of algebraic constraints. The constraint we derive may be called the expansion equation and is discussed in this paper.

Apart from a standard, two-stage scheme [6], a three-stage scheme is formulated. Some simple mathematical properties of the two schemes are presented, after which the two schemes are

compared in a numerical example. In this example, the three-stage scheme produces more stable results than the two-stage scheme.

In Section 2 of this paper, the governing equations for laminar combustion are presented. Subsequently, in Section 3, the space discretized conservation equations are written in differential algebraic form. This system is reformulated to its semi-explicit form in Section 4, by deriving the constraint equations. The two pressure correction schemes are presented in Section 5, and furthermore a brief discussion of the available literature is presented in Section 5.4. An analysis for large time steps is presented in Section 6. Finally, in Section 7, the theory is verified in a numerical example of a two-dimensional Bunsen flame.

2 Governing Equations

A laminar flame can be considered as the flow of a reacting gas mixture. Therefore, a rigorous mathematical model for laminar flames is based on the kinetic theory of reactive gases. However, the kinetic model is often too complicated to solve, and therefore simplifications are needed, which are appropriate for laminar flames. It is beyond the scope of this paper to make a thorough investigation of laminar flame models, instead we present the model used in [10, 13]. Laminar flames in an open environment can be described by the following conservation equations for the mass density ρ, the velocity $\boldsymbol{v}$, the temperature T and all but one of the N_s species' mass fractions Y_j:

$$\frac{\partial \rho}{\partial t} = -\nabla \cdot (\rho \boldsymbol{v}), \tag{2.1a}$$

$$\frac{\partial \boldsymbol{v}}{\partial t} = -(\boldsymbol{v} \cdot \nabla)\boldsymbol{v} + \boldsymbol{g} - \frac{1}{\rho}\nabla p + \frac{1}{\rho}\nabla \cdot \left(\mu \left(\nabla \boldsymbol{v} + (\nabla \boldsymbol{v})^T - \frac{2}{3}\boldsymbol{I}(\nabla \cdot \boldsymbol{v})\right)\right), \tag{2.1b}$$

$$\frac{\partial T}{\partial t} = -\boldsymbol{v} \cdot \nabla T + \frac{1}{c_p \rho}\nabla \cdot (\lambda \nabla T) - \frac{1}{c_p \rho}\sum_{j=1}^{N_s} c_{pj} Y_j \boldsymbol{V}_j \cdot \nabla T + s_T, \tag{2.1c}$$

$$\frac{\partial Y_j}{\partial t} = -\boldsymbol{v} \cdot \nabla Y_j - \frac{1}{\rho}\nabla \cdot (\rho Y_j \boldsymbol{V}_j) + s_j, \quad i = 1, \cdots N_s - 1, \tag{2.1d}$$

with gravitational acceleration $\boldsymbol{g}$, pressure p, viscosity coefficient μ, thermal conductivity coefficient λ, specific heat c_p, specific heat of j-th species c_{pj}, j-th species' diffusion velocity $\boldsymbol{V}_j$, thermal production term s_T and reactive source term s_j.

The system (2.1) has to be completed with models for μ, λ, c_p, c_{pj}, s_T, s_j and $\boldsymbol{V}_j$. For the diffusion velocities $\boldsymbol{V}_j$, we use the generalized Fick's Law [8] for the species numbered 1 to $N_s - 1$. Moreover, the total diffusion of mass must be zero. Thus we obtain

$$Y_j \boldsymbol{V}_j = -\frac{\lambda}{\rho c_p Le_j}\nabla Y_j, \quad (j = 1, \cdots, N_s - 1), \qquad \sum_{j=1}^{N_s} Y_j \boldsymbol{V}_j = 0. \tag{2.2a}$$

The Lewis numbers $Le_1, \cdots, Le_{N_s-1}$ are assumed constant. We like to emphasize that the pressure correction methods to be introduced in Section 5, do not depend on this particular model for the diffusion velocities.

The viscosity coefficient μ, the conduction coefficient λ, the specific heat c_p, the chemical reaction terms $s_1, s_2, \cdots, s_{N_s-1}$ and the chemical heat production term s_T are all given by constitutive equations of the form [13]

$$\mu = \mu(T, Y_1, \cdots, Y_{N_s}), \qquad \lambda = \lambda(T, Y_1, \cdots Y_{N_s}), \qquad c_p = \sum_{j=1}^{N_s} Y_j c_{pj}(T), \tag{2.2b}$$

$$s_j = s_j(T, Y_1, \cdots, Y_{N_s}), \quad s_T = s_T(T, Y_1, \cdots, Y_{N_s}). \tag{2.2c}$$

Measurements [7] are performed to obtain realistic expressions for these constitutive relationships. Furthermore, the mass fractions Y_j must add up to 1:

$$\sum_{j=1}^{N_s} Y_j = 1. \tag{2.2d}$$

Finally, to close the system, we need the thermal equation of state, given by

$$\rho = \frac{p_0 M}{RT}, \quad \text{with} \quad \frac{1}{M} = \sum_{j=1}^{N_s} \frac{Y_j}{M_j}. \tag{2.2e}$$

The average molecular mass M is thus given as the reciprocal, weighted average of the (constant) molecular masses $M_1, \cdots, M_{N_s}$. R is known as the universal gas constant. Since laminar flames exist under almost isobaric conditions, the ambient pressure p_0 is considered constant. This model does not describe acoustic phenomena.

In the following sections we shall reformulate this system, in order to analyze its mathematical nature, and explain the troubles arising in its numerical solution. This will then lead to new pressure correction schemes, which remedy these problems.

3 Semi-Discrete Formulation of the Combustion Problem

Using equations (2.2a-e), all quantities except the temperature T, the pressure p, the velocity $\boldsymbol{v}$ and the mass fractions $Y_1, \cdots, Y_{N_s-1}$ may be eliminated from the system (2.1a-d). After space discretization, using e.g. a finite volume scheme on a staggered grid, the system (2.1a-d) yields a system, which we will later show to be a system of differential algebraic equations (DAEs). Now, let us introduce some notation in order to study the structure of the DAE system. The equations involve three large vectors of unknowns. The first one, $\boldsymbol{\phi} \in \mathbb{R}^{NN_s}$ (N is the grid size), contains the approximate temperatures and mass fractions in all of the N grid nodes. The second vector, $\boldsymbol{v} \in \mathbb{R}^{2N}$ (assuming a two-dimensional problem) contains the approximate velocity components, and $\boldsymbol{p} \in \mathbb{R}^N$ contains the approximate pressure levels.

The combined temperature equation (2.1c) and species conservation equations (2.1d), after space discretization, yield the time derivative $\frac{\mathrm{d}\boldsymbol{\phi}}{\mathrm{d}t}$, in terms of $\boldsymbol{\phi}$ and $\boldsymbol{v}$. The equation is linear in $\boldsymbol{v}$, and can be written as

$$\frac{\mathrm{d}\boldsymbol{\phi}}{\mathrm{d}t} = A_1(\boldsymbol{\phi}) + \mathcal{A}_2(\boldsymbol{\phi})\boldsymbol{v}. \tag{3.1a}$$

Different types of fonts are used for $A_1 : \mathbb{R}^{NN_s} \to \mathbb{R}^{NN_s}$ and $\mathcal{A}_2 : \mathbb{R}^{NN_s} \to \mathbb{R}^{NN_s \times 2N}$, because A_1 can be considered a function and $\mathcal{A}_2$ an operator. We will use this convention throughout the paper.

The momentum equations (2.1b) yield the time derivative $\frac{\mathrm{d}\boldsymbol{v}}{\mathrm{d}t}$ in terms of $\boldsymbol{\phi}$, $\boldsymbol{v}$ and $\boldsymbol{p}$. It is linear in $\boldsymbol{p}$, and can be written as

$$\frac{\mathrm{d}\boldsymbol{v}}{\mathrm{d}t} = B_1(\boldsymbol{\phi}, \boldsymbol{v}) + \mathcal{B}_2(\boldsymbol{\phi})\boldsymbol{p}. \tag{3.1b}$$

Last, the continuity equation expresses the time derivative of the density, which is a function of $\boldsymbol{\phi}$ (through the equation of state 2.2e), in terms of $\boldsymbol{\phi}$ and $\boldsymbol{v}$. Again, the equation is linear in $\boldsymbol{v}$, say

$$\frac{\mathrm{d}Q(\boldsymbol{\phi})}{\mathrm{d}t} = \mathcal{C}(\boldsymbol{\phi})\boldsymbol{v}. \tag{3.1c}$$

In this paper, first the mathematical nature of the system (3.1a-c) is determined, and then some accurate and efficient time integration schemes can be constructed to solve (3.1a-c) numerically.

4 DAE Structure of the Combustion Problem

In this section, we shall further investigate the mathematical properties of system (3.1a-c), and we shall show that it can be classified as a constrained or differential algebraic system.

From equation (3.1c), we may derive

$$\frac{\partial Q}{\partial \phi}\frac{\mathrm{d}\phi}{\mathrm{d}t} = C(\phi)v, \tag{4.1}$$

and after substitution of (3.1a), all time derivatives disappear:

$$\left(C(\phi) - \frac{\partial Q}{\partial \phi}\mathcal{A}_2(\phi)\right)v = \frac{\partial Q}{\partial \phi}A_1(\phi). \tag{4.2}$$

We can abbreviate this as

$$\mathcal{P}_1(\phi)v = P_2(\phi). \tag{4.3}$$

We call this equation the constraint between v and ϕ, because it prevents the solution to move freely through the space of all possible solutions. Instead, it will always be in the (lower dimensional) subspace of all the possible solutions which satisfy (4.3).

Taking the time derivative of both left and right-hand sides in the constraint (4.3), we obtain

$$\mathcal{P}_1(\phi)\frac{\mathrm{d}v}{\mathrm{d}t} + \left(\frac{\partial \mathcal{P}_1}{\partial \phi}\frac{\mathrm{d}\phi}{\mathrm{d}t}\right)v = \frac{\partial P_2}{\partial \phi}\frac{\mathrm{d}\phi}{\mathrm{d}t}. \tag{4.4}$$

Note that the Frechet derivative $\frac{\partial \mathcal{P}_1}{\partial \phi}(\phi) : I\!R^{NN_s} \rightarrow I\!R^{NN_s \times 2N}$ is a tensor (operator) of third order. After substitution of (3.1a-b), it is seen that

$$\mathcal{L}_1(\phi)p = L_2(\phi, v), \tag{4.5}$$

with

$$\mathcal{L}_1(\phi) = \mathcal{P}_1(\phi)\mathcal{B}_2(\phi), \tag{4.6a}$$

$$L_2(\phi, v) = \frac{\partial P_2}{\partial \phi}\left(A_1(\phi) + \mathcal{A}_2(\phi)v\right) - \mathcal{P}_1(\phi)B_1(\phi, v) - \left(\frac{\partial \mathcal{P}_1}{\partial \phi}\left(A_1(\phi) + \mathcal{A}_2(\phi)v\right)\right)v. \tag{4.6b}$$

Equation (4.5) is known as the pressure equation [6], or sometimes as the hidden constraint [12]. In the cases of interest, it can be solved to determine the pressure. It expresses therefore the fact that the pressure can be eliminated from the system, as it follows directly from the other variables. Note that the constraint equation (4.3)does not hold when the isobaric approximation is not made, i.e. when the factor p_0 in (2.2e) is replaced by p. The resulting system is then unconstrained. Since the Mach numbers in the combustion problems we consider are extremely small, however, the behavior of the system will be similar to that of the constrained equations.

We shall now illustrate the theory of this section by applying it to a concrete example, in which we derive the constraint and the pressure equation for the two-dimensional, incompressible Navier-Stokes equations.

Example 4.1 Consider the two-dimensional incompressible Navier-Stokes equations

$$\frac{\partial v}{\partial t} = -v \cdot \nabla v + \mu \nabla^2 v - \nabla p, \tag{4.7a}$$

$$\nabla \cdot v = 0. \tag{4.7b}$$

The continuity equation (4.7b) now contains no temporal derivatives and is therefore the constraint. Taking the time derivative of the flow field divergence, and assuming the viscosity coefficient μ to be constant, we find

$$\nabla^2 p = -\nabla u \cdot \frac{\partial \boldsymbol{v}}{\partial x} - \nabla v \cdot \frac{\partial \boldsymbol{v}}{\partial y}. \tag{4.8}$$

Equation (4.8) now represents the pressure equation (4.5).

Thus, the solution -which consists of the three scalar fields u, v and p- moves through the subspace of those fields which satisfy both (4.7b) and (4.8).

The technique of applying differentiation to the constraint in order to derive the pressure equation is known as the index reduction technique, used in DAE literature for the time integration of constrained systems of differential equations [5].

Even in the case of combustion phenomena, the constraint equation can be written in a more explicit form than (4.3). For the combustion equations (2.1a-d), the constraint equation (4.3) can be shown to be equivalent to a space discretization of

$$\rho \nabla \cdot \boldsymbol{v} = \frac{1}{c_p T} \nabla \cdot (\lambda \nabla T) + \frac{\rho s_T}{T} - \frac{1}{T} \nabla T \cdot \sum_{j=1}^{N_s} \frac{c_{pj}}{c_p} Y_j \boldsymbol{V}_j + \sum_{j=1}^{N_s} \frac{M}{M_j} (\rho s_j - \nabla \cdot (\rho Y_j \boldsymbol{V}_j)). \tag{4.9}$$

Recall that $\boldsymbol{V}_j$ denotes the diffusion flow velocity of species number j. Let us investigate the meaning of these terms. The left hand side is the expansion rate, which can be seen by writing the continuity equation as

$$\frac{D\rho}{Dt} = -\rho \nabla \cdot \boldsymbol{v}. \tag{4.10}$$

The terms on the right hand side of the equation each denote a physical phenomenon which may cause expansion in a gas. The first three terms in the right hand side are heating terms. The first term describes the heating of the gas due to conduction, the second term the heating due to chemical reactions. The third term is the heating effect due to diffusive mixing. The last term in (4.9) describes the expansion due to a change in average molecular mass, either through chemical reactions, or through mass diffusion.

The pressure equation (4.5) is not elaborated, because it is very complex, yet provides no extra information. It must be noted, however, that a pressure equation exists, determining the pressure instantaneously as a dependent variable of $\boldsymbol{\phi}$ and $\boldsymbol{v}$.

In the following sections, we shall study the implications which the existence of constraints has for numerical time integration using a pressure correction scheme.

5 Pressure Correction

5.1 Two-Stage Pressure Correction Scheme

Pressure correction is a powerful approach to the numerical integration of systems which have the form (3.1a-c). Before introducing the pressure correction methods, we study the Euler Backward time integration scheme. For the system (3.1a-c), Euler Backward time integration defines a sequence of solutions $(\boldsymbol{\phi}_0, \boldsymbol{v}_0, \boldsymbol{p}_0), \cdots, (\boldsymbol{\phi}_k, \boldsymbol{v}_k, \boldsymbol{p}_k)$, with

$$\boldsymbol{\phi}_k = \boldsymbol{\phi}(k\Delta t) + \mathcal{O}(\Delta t), \quad \boldsymbol{v}_k = \boldsymbol{v}(k\Delta t) + \mathcal{O}(\Delta t), \quad \boldsymbol{p}_k = \boldsymbol{p}(k\Delta t) + \mathcal{O}(\Delta t). \tag{5.1}$$

These approximations are defined by the recursive relations

$$\frac{\boldsymbol{\phi}_n - \boldsymbol{\phi}_{n-1}}{\Delta t} = A_1(\boldsymbol{\phi}_n) + A_2(\boldsymbol{\phi}_n)\boldsymbol{v}_n, \tag{5.2a}$$

$$\frac{\boldsymbol{v}_n - \boldsymbol{v}_{n-1}}{\Delta t} = B_1(\boldsymbol{\phi}_n, \boldsymbol{v}_n) + B_2(\boldsymbol{\phi}_n)\boldsymbol{p}_n, \tag{5.2b}$$

$$\frac{Q(\boldsymbol{\phi}_n) - Q(\boldsymbol{\phi}_{n-1})}{\Delta t} = C(\boldsymbol{\phi}_n)\boldsymbol{v}_n. \tag{5.2c}$$

Note that this is a straightforward application of the Euler Backward time integration scheme as it is used for ordinary differential equations (ODEs), and that the results of Section 4 are not used at all. If Q were a linear function, we could derive the constraint equation (4.3) for time levels $n = 1, 2, \cdots$ by substitution of (5.2a) into (5.2c). If $\mathcal{P}_1$ and P_2 were also linear, combination of the constraint equation (4.3) on two consecutive time levels would yield the pressure equation (4.5) for time levels $n = 2, 3, \cdots$. Moreover, it can be shown that, for all linear systems of the form (3.1a-c), the Euler Backward approximation (5.2a-c) yields stable solutions (i.e. $\boldsymbol{\phi}_k$, $\boldsymbol{v}_k$, and $\boldsymbol{p}_k$ converge to stationary values for $k \to +\infty$), if (3.1a-c) does (i.e. if $\boldsymbol{\phi}(t)$, $\boldsymbol{v}(t)$, and $\boldsymbol{p}(t)$ converge to stationary values for $t \to +\infty$). Thus, without using Section 4, a reliable time integration scheme is obtained. A big problem in the application of the Euler Backward scheme, however, is that its implementation requires the solution of (5.2a-c) as a coupled system of equations for $\boldsymbol{\phi}_n$, $\boldsymbol{v}_n$ and $\boldsymbol{p}_n$. System (5.2a-c) is essentially more difficult to solve than the equations obtained for an ODE system, due to the constraints which are hidden inside it. Note that it is not the number of unknowns in the equation, but its mathematical structure which makes it so hard to solve. To circumvent the solution of (5.2a-c), pressure correction algorithms have been introduced.

Many of the ideas in this paper are derived from the work of Issa [6], but modifications have proven necessary. Pressure correction schemes produce an approximation for the solution at a new time level, by consecutive solution of systems which are easier than (5.2a-c). This is done by first calculating predictor values for some of the variables, after which these are made to satisfy the constraint equation (4.3) by projection. A variety of methods can be formulated by varying the number of predictor-corrector iterations. Accuracy can be enhanced by construction of higher order time integration methods. Here, we will study first-order methods only, and our concern will mainly be one of stability rather than accuracy.

As a starting point, we shall apply a simple two-stage pressure correction scheme to system (3.1a-c). This yields

$$\frac{\boldsymbol{\phi}_n - \boldsymbol{\phi}_{n-1}}{\Delta t} = A_1(\boldsymbol{\phi}_n) + \mathcal{A}_2(\boldsymbol{\phi}_n)\boldsymbol{v}_*, \tag{5.3a}$$

$$\frac{\boldsymbol{v}_* - \boldsymbol{v}_{n-1}}{\Delta t} = B_1(\boldsymbol{\phi}_n, \boldsymbol{v}_*) + \mathcal{B}_2(\boldsymbol{\phi}_n)\boldsymbol{p}_{n-1}, \tag{5.3b}$$

$$\frac{\boldsymbol{v}_n - \boldsymbol{v}_{n-1}}{\Delta t} = B_1(\boldsymbol{\phi}_n, \boldsymbol{v}_*) + \mathcal{B}_2(\boldsymbol{\phi}_n)\boldsymbol{p}_n, \tag{5.3c}$$

$$\mathcal{P}_1(\boldsymbol{\phi}_n)\boldsymbol{v}_n = P_2(\boldsymbol{\phi}_n). \tag{5.3d}$$

Note that in the pressure correction scheme we use the constraint equation (5.3d), where for the Euler Backward scheme it was sufficient to use the discrete continuity equation (5.2c). In Theorem 5.1 we will provide argumentation for this difference.

The the new values $\boldsymbol{\phi}_n$, $\boldsymbol{v}_n$ and $\boldsymbol{p}_n$ defined in (5.3a-d) can be found much more easily than the new values for the Euler Backward scheme (5.2a-c), because we can decouple the pressure from the other variables. To do so, we first combine (5.3b-c) to derive

$$\boldsymbol{v}_n = \boldsymbol{v}_* + \Delta t \mathcal{B}_2(\boldsymbol{\phi}_n)(\boldsymbol{p}_n - \boldsymbol{p}_{n-1}). \tag{5.4}$$

Next, we combine (5.4) and (5.3d) to derive

$$\Delta t \mathcal{P}_1(\boldsymbol{\phi}_n)\mathcal{B}_2(\boldsymbol{\phi}_n)(\boldsymbol{p}_n - \boldsymbol{p}_{n-1}) = P_2(\boldsymbol{\phi}_n) - \mathcal{P}_1(\boldsymbol{\phi}_n)\boldsymbol{v}_*. \tag{5.5}$$

The new values $\boldsymbol{\phi}_n$, $\boldsymbol{v}_n$ and $\boldsymbol{p}_n$, defined in (5.3a-d) can be found in the following two steps.

1. Calculate $\boldsymbol{\phi}_n$ and $\boldsymbol{v}_*$ by solving (5.3a-b) in a coupled way.
2. Solve (5.5) for $\boldsymbol{p}_n$ and update $\boldsymbol{v}_n$ from (5.4).

These two steps are indeed easier than the implicit step necessary for e.g. Euler Backward time integration (5.2a-c). In step 1, an equation is solved like the ones found in an implicit time step for an unconstrained system. Equation (5.5) is a linear equation, involving only a scalar field. Such equations can be solved efficiently using standard techniques. Equation (5.4), finally, involves

nothing but the substitution of $\boldsymbol{p}_n$. Thus, step 1 and step 2 require computational effort, but considerably less than necessary for Euler Backward time stepping.

Following the approach of the pressure correction scheme (5.3a-d), the numerical solution will, like the exact solution of the semi-discrete system (3.1a-c), always be a point in the subspace of all possible solutions which satisfy the constraint equation. The pressure equation (4.5), however, is not explicitly imposed. This implies that the numerical solution, unlike the exact solution, depends on the initial conditions for the pressure. The numerical solution has a larger subspace for its domain than the exact solution of the semi-discrete system. We shall come back to this in Section 5.3.

The current pressure correction scheme, (5.3a-d), differs in an important way from what is commonly used, because we use the constraint equation in (5.3d), instead of the continuity equation. In the following subsection, we shall discuss the reasons for this difference.

5.2 Constraint, not Continuity

The last equation in the two-stage pressure correction scheme, (5.3d), is an implicit formulation of the constraint equation. It is very common to use, instead, the continuity equation, which yields the following pressure correction scheme

$$\frac{\boldsymbol{\phi}_n - \boldsymbol{\phi}_{n-1}}{\Delta t} = A_1(\boldsymbol{\phi}_n) + \mathcal{A}_2(\boldsymbol{\phi}_n)\boldsymbol{v}_*, \tag{5.6a}$$

$$\frac{\boldsymbol{v}_* - \boldsymbol{v}_{n-1}}{\Delta t} = B_1(\boldsymbol{\phi}_n, \boldsymbol{v}_*) + \mathcal{B}_2(\boldsymbol{\phi}_n)\boldsymbol{p}_{n-1}, \tag{5.6b}$$

$$\frac{\boldsymbol{v}_n - \boldsymbol{v}_{n-1}}{\Delta t} = B_1(\boldsymbol{\phi}_n, \boldsymbol{v}_*) + \mathcal{B}_2(\boldsymbol{\phi}_n)\boldsymbol{p}_n, \tag{5.6c}$$

$$\frac{Q(\boldsymbol{\phi}_n) - Q(\boldsymbol{\phi}_{n-1})}{\Delta t} = C(\boldsymbol{\phi}_n)\boldsymbol{v}_n. \tag{5.6d}$$

The reason for the widespread use of (5.6a-d) is probably twofold. First, the usual formulation of the model is (2.1a-d) and includes a continuity equation, not a constraint equation. Second, the pressure correction schemes have been developed originally for the incompressible Navier-Stokes equations (4.7a-b), for which the continuity equation is the constraint.

However, the use of pressure correction scheme (5.6) should be strongly advised against. The following theorem provides the reason why.

Theorem 5.1 *There are stable systems of the form (3.1a-c), for which the pressure correction scheme (5.6a-d) produces unstable results, even for $\Delta t \to 0$. Thus, the solution of (3.1a-c) fulfills*

$$\lim_{t\to\infty} \boldsymbol{\phi}(t) = \boldsymbol{\phi}_\infty, \quad \lim_{t\to\infty} \boldsymbol{v}(t) = \boldsymbol{v}_\infty, \quad \lim_{t\to\infty} \boldsymbol{p}(t) = \boldsymbol{p}_\infty, \tag{5.7}$$

with $\|\boldsymbol{\phi}_\infty\| < \infty$, $\|\boldsymbol{v}_\infty\| < \infty$, $\|\boldsymbol{p}_\infty\| < \infty$. The corresponding solution of (5.6a-d), on the contrary, has

$$\lim_{n\to+\infty} \|\boldsymbol{\phi}_n\| = \lim_{n\to+\infty} \|\boldsymbol{v}_n\| = \lim_{n\to+\infty} \|\boldsymbol{p}_n\| = +\infty, \tag{5.8}$$

even for arbitrarily small time step $\Delta t > 0$.

Proof: An example of such a system is given by

$$\frac{\mathrm{d}\phi}{\mathrm{d}t} = -2\phi + v, \quad \frac{\mathrm{d}v}{\mathrm{d}t} = -\phi - v + p, \quad \frac{\mathrm{d}\phi}{\mathrm{d}t} = -v. \tag{5.9}$$

It is easily verified that the solution is given by

$$\phi = v = p = C\exp(-t), \tag{5.10}$$

where C is some constant determined by the initial condition. Obviously, this is stable in the meaning of (5.7).

The pressure correction scheme (5.6a-d) produces solutions according to the recursion relation

$$\begin{pmatrix} \phi_n \\ v_n \\ \Delta t p_n \end{pmatrix} = A(\Delta t) \begin{pmatrix} \phi_{n-1} \\ v_{n-1} \\ \Delta t p_{n-1} \end{pmatrix}, \tag{5.11}$$

with

$$A(\Delta t) := \frac{1}{1+3\Delta t+3\Delta t^2} \begin{pmatrix} 1+\Delta t & \Delta t & \Delta t \\ 2+3\Delta t & -1 & -1 \\ 2+4\Delta t & -(2+2\Delta t) & -(1-\Delta t-3\Delta t^2) \end{pmatrix}. \tag{5.12}$$

The eigenvalues of $A(\Delta t)$ are given by

$$\sigma(A(\Delta t)) = \left\{1+\mathcal{O}(\Delta t), -1+\sqrt{2}+\mathcal{O}(\Delta t), -1-\sqrt{2}+\mathcal{O}(\Delta t)\right\}, \tag{5.13}$$

and since $-1-\sqrt{2} < -1$, we have (5.8). □

It must be noted here that the system (5.10) has no direct connection to the combustion problem. Its function is to help prove Theorem 5.1, which clearly has a connection to combustion phenomena. The instabilities, which the theorem predicts for continuity-based pressure correction methods, have actually been observed in numerical calculations of two-dimensional, laminar Bunsen flames.

For Euler Backward and for the two-stage pressure correction scheme (5.3a-c), stability for small enough time steps can be proven for stable linear systems.

5.3 Three-Stage Pressure Correction Scheme

An interesting suggestion done by Issa in [6], is the use of a three-stage pressure correction scheme instead of a two-stage scheme. He claims that a much better treatment of the pressure equation is obtained that way, at least for the incompressible Navier-Stokes equations. A suitable generalization of this idea for the case of combustion simulation can only be made on the basis of the analysis of the constraints as presented in this chapter.

It would definitely have advantages if one could simply impose the pressure equation (4.5) after every time step, eliminating the pressure as a variable. The resulting three-stage scheme would then be

$$\frac{\boldsymbol{\phi}_n - \boldsymbol{\phi}_{n-1}}{\Delta t} = A_1(\boldsymbol{\phi}_n) + A_2(\boldsymbol{\phi}_n)\boldsymbol{v}_*, \tag{5.14a}$$

$$\frac{\boldsymbol{v}_* - \boldsymbol{v}_{n-1}}{\Delta t} = B_1(\boldsymbol{\phi}_n, \boldsymbol{v}_*) + B_2(\boldsymbol{\phi}_n)\boldsymbol{p}_{n-1}, \tag{5.14b}$$

$$\frac{\boldsymbol{v}_n - \boldsymbol{v}_{n-1}}{\Delta t} = B_1(\boldsymbol{\phi}_n, \boldsymbol{v}_*) + B_2(\boldsymbol{\phi}_n)\boldsymbol{p}_*, \tag{5.14c}$$

$$\mathcal{P}_1(\boldsymbol{\phi}_n)\boldsymbol{v}_n = P_2(\boldsymbol{\phi}_n), \tag{5.14d}$$

$$\mathcal{L}_1(\boldsymbol{\phi}_n)\boldsymbol{p}_n = L_2(\boldsymbol{\phi}_n, \boldsymbol{v}_n). \tag{5.14e}$$

We will now discuss the reasons why this scheme may be more accurate and stable than the two-stage scheme (5.3a-d), while the time steps still require less computing effort than the Euler Backward time steps of (5.2a-c).

Because of the explicit form in which the pressure equation is now imposed, the numerical solution now moves through the same subspace of all the possible solutions which satisfy the constraint equation and the pressure equation. In that sense it is more like the exact solution than the numerical solution of (5.3a-d). This is the reason why (5.14a-e) may be more accurate and stable than the two-stage scheme (5.3a-d).

Next, we discuss the implementation of the scheme. The complicated form of the function L_2 in (4.5) makes it inefficient to solve it in a straightforward way. Instead, we use the following steps. The values $\boldsymbol{v}_n$, $\boldsymbol{\phi}_n$ and $\boldsymbol{p}_*$ can be obtained by performing the same steps as were necessary for the

two-stage scheme, the only difference of course being that what was called the 'new pressure' $\boldsymbol{p}_n$ in the two-stage scheme is now called the 'intermediate pressure' $\boldsymbol{p}_*$.

To calculate the new pressure $\boldsymbol{p}_n$, we define the intermediate values $\boldsymbol{\phi}_*$ and $\boldsymbol{v}_{**}$ by

$$\boldsymbol{\phi}_* := \boldsymbol{\phi}_n - A_1(\boldsymbol{\phi}_n)\Delta t - A_2(\boldsymbol{\phi}_n)\boldsymbol{v}_n\Delta t, \tag{5.15a}$$

$$\boldsymbol{v}_{**} := \boldsymbol{v}_n - B_1(\boldsymbol{\phi}_n, \boldsymbol{v}_n)\Delta t - B_2(\boldsymbol{\phi}_n)\boldsymbol{p}_*\Delta t. \tag{5.15b}$$

This is a negative step in time, and can be trivially solved for the intermediate values.

With these values, $\boldsymbol{p}_n$ can be solved from the following system

$$\Delta t\mathcal{P}_1(\boldsymbol{\phi}_*)\mathcal{B}_2(\boldsymbol{\phi}_*)(\boldsymbol{p}_n - \boldsymbol{p}_*) = P_2(\boldsymbol{\phi}_n) - \mathcal{P}_1(\boldsymbol{\phi}_n)\boldsymbol{v}_n + \mathcal{P}_1(\boldsymbol{\phi}_*)\boldsymbol{v}_{**} - P_2(\boldsymbol{\phi}_*). \tag{5.16}$$

Equation (5.16) is very similar to the pressure correction equation (5.5), and since the two-stage algorithm can be done cheaply, so can the three-stage algorithm. By combination of (5.15a-b) and the definition of $\mathcal{L}_1$ and L_2, it can be shown that the pressure field $\boldsymbol{p}_n$, thus obtained, satisfies the pressure equation (5.14e), where the partial derivatives $\frac{\partial \mathcal{P}_1}{\partial \phi}$ and $\frac{\partial P_2}{\partial \phi}$ in L_2 have been replaced by their first order difference quotients. This is exact if the system is linear. For nonlinear systems, the pressure equation is only solved to first order accuracy.

The three-stage scheme can be written in the following simple steps.

1. Calculate $\boldsymbol{\phi}_n$ and $\boldsymbol{v}_*$ from (5.14a-b).
2. Solve (5.5), with $\boldsymbol{p}_n$ replaced by $\boldsymbol{p}_*$, for the intermediate pressure $\boldsymbol{p}_*$. Update $\boldsymbol{v}_n$ from (5.4), with $\boldsymbol{p}_n$ replaced by $\boldsymbol{p}_*$.
3. Calculate $\boldsymbol{\phi}_*$ and $\boldsymbol{v}_{**}$ from (5.15a-b). Solve (5.16), for the new pressure $\boldsymbol{p}_n$.

5.4 Comparison of Pressure Correction Schemes

Introduced in 1967 by Chorin [3], pressure correction schemes have been a topic of research for over thirty years. In this section, a brief account is given of the main developments in the area and an indication will be given of the main difference between the current approach and the approaches of earlier work.

The first pressure correction scheme [3] dealt with the time integration of systems obtained from discretized Navier-Stokes equations. It is similar to the two-stage scheme (5.3a-d), with the exception that the pressure term is not included at all in the predictor step. Thus, the predictor step is not a consistent time step, and moreover, a stationary solution which may be found depends on the time step Δt.

A contemporary of Chorin, Temam [11], introduced a very similar scheme. This scheme is also very similar to (5.3a-d), yet it treats the predictor step with an explicit time integration step rather than an implicit one.

The application of pressure correction methods to stationary problems is discussed by Patankar [9] in 1972, where the very popular SIMPLE-type methods find their origin. We address the issue of finding stationary solutions briefly in Section 6.

New work was presented by Issa in 1985 [6]. A three-stage pressure corrrection method was presented which was reported to produce much more accurate pressure fields than did the available methods up to that time. The three-stage method was not, however, based on the pressure equation (4.5) but it was presented as an iterative method for the solution of the Backward Euler equations (5.2a-c), using two iterations. Generalizations are proposed for the application of the pressure correction schemes to compressible and variable temperature systems, including the current application. No use is made, however, of the expansion equation (4.9), so the resulting method for the combustion system is very close to the continuity correction method (5.6a-d), which we proved to be unstable. Gresho and Chan present a general formulation for pressure correction methods (for the incompressible Navier-Stokes equations), first published in 1988, of which the current application can be seen a special case. It can be found in [4]. Though the reformulation of the combustion equations using the expansion equation (4.9) is known (and used in e.g. [2]),

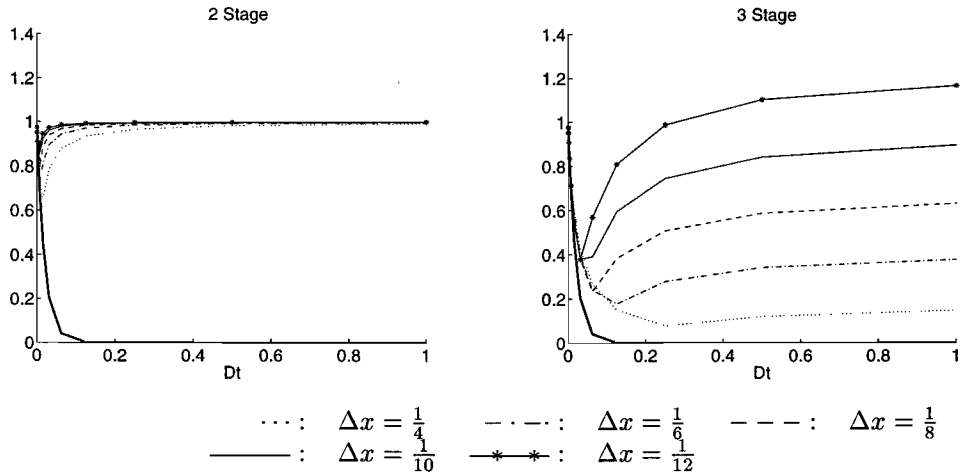

Figure 1: Spectral radius of the two-stage method (left) and the three-stage method (right), for the two-dimensional Stokes problem. Bold lines indicate the exact solution.

its importance for the use in pressure correction schemes has not been pointed out in any of the work known to us. The scheme presented in [1] concerns the application of pressure correction to systems with density variations due to pressure variations.

Apart from the earlier mentioned scheme, also some more recent work is discussed in [4]. All this work is concentrated on the derivation of convergence results, and the construction of higher order methods. Convergence results are very hard to obtain, mostly due to the fact that the corrected velocity $\boldsymbol{v}_n$ does not satisfy all of the boundary conditions.

6 Large Time Step Behavior

In the -common- case that time steps are used to find a stationary solution, and also in the case that very slow processes are studied, the time steps may be very large. The Euler Backward scheme provides enough numerical damping to be reliable in such cases, but is, as pointed out, very difficult to implement. The behavior of the pressure correction schemes (5.3a-d) and (5.14a-e) for large time steps is not easily assessed. It is, for example, possible to construct systems for which these schemes become unstable, or remain stable for large time steps. They do so independently of each other.

There is, however, one difference between the two schemes which can easily be derived, and may shed some light on their respective long time step behavior. For $\Delta t \to +\infty$, we have $\boldsymbol{p}_n = \boldsymbol{p}_{n-1}$ from (5.5). Therefore, the two-stage scheme provides hardly any damping when a very large time step is taken. The behavior of the three stage scheme does not exhibit this stagnation phenomenon for large time steps. We shall now further illustrate this with an example.

Example 6.1 In order to compare the two schemes, let us apply them to a very simple flow equation. Consider the two-dimensional Stokes problem

$$\frac{\partial \boldsymbol{v}}{\partial t} = \nabla^2 \boldsymbol{v} - \nabla p \quad , \quad \nabla \cdot \boldsymbol{v} = 0, \tag{6.1a}$$

$$\boldsymbol{v}|_{\partial\Omega} = 0 \quad , \quad \int_{\Omega} p \, \mathrm{d}\Omega = 0, \tag{6.1b}$$

where the last equation determines a unique pressure. We discretize in space using the central difference based finite volume method on a staggered grid, and apply the two

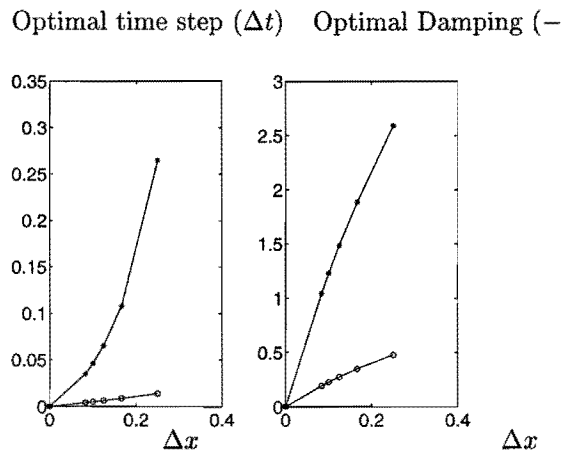

Figure 2: Optimal time step (left) and damping (right) as a function of the grid size Δx. Stars indicate the results of the three-step method; circles of the two-stage method.

pressure correction schemes. The stationary solution is of course

$$u = v = p = 0. \tag{6.2}$$

The problem is linear, so a *transition* matrix $\boldsymbol{A}(\Delta t)$ exists, for which

$$\begin{pmatrix} u_n \\ v_n \\ p_n \end{pmatrix} = \boldsymbol{A}(\Delta t) \begin{pmatrix} u_{n-1} \\ v_{n-1} \\ p_{n-1} \end{pmatrix}. \tag{6.3}$$

Since the continuity equation and the expansion equation are, in this case, identical, there is no difference between the two-stage and the continuity pressure correction method. Thus, we can only compare the two and three-stage schemes. In Figure 1, the spectral radius $\rho(\boldsymbol{A}(\Delta t))$ of the matrix $\boldsymbol{A}(\Delta t)$ is given for the two methods.

The two-stage scheme is unconditionally stable, and the spectral radius is very close to that of the exact solution for small Δt, indicating time accuracy for simulations with small time steps. For large time steps, however, the spectral radius quickly approaches one. The time step at which this effect appears is proportional to the mesh size Δx. The results of the three-stage scheme, differ a lot from the behavior of the two-step scheme. The spectral radius does not converge to zero as the time step becomes larger: instead, it converges to a value which is inversely proportional to the mesh size ($\rho(\boldsymbol{A}(\infty)) = \mathcal{O}(\Delta x^{-1})$), so the three-stage scheme is not unconditionally stable for fine grids. The maximum damping which can be obtained for a carefully chosen time step, however, is a lot stronger than is possible with the two-stage scheme, making it possible to obtain a stationary solution in much fewer time steps than with the two-stage scheme. This can be seen from Figure 2, where the time step with optimal damping, as well as the optimal damping itself, is given as a function of the grid size Δx.

7 Numerical Example

As a test case for the pressure correction schemes of this paper, we do a simulation of a single slit burner. The solution is assumed two-dimensional and symmetric relative to the center of

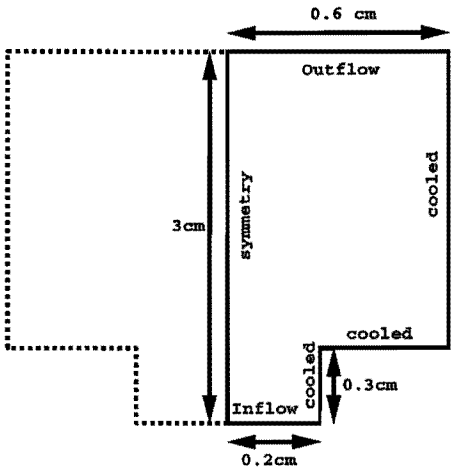

Figure 3: The computational domain

the burner, which we take to be the y-axis. The computational domain is shown in Figure 3. Different boundary conditions are imposed at each boundary. At the inflow, the following boundary conditions are imposed for the velocity $\boldsymbol{v} = (u, v)^T$, the temperature T and the mass fractions Y_j:

$$v = v_0 \left(1 - \left(\frac{x}{0.2}\right)^2\right), \quad u = 0, \quad T = 327K, \tag{7.1a}$$

$$Y_j = Y_{j0}, \qquad j = 1, \cdots, N_s - 1. \tag{7.1b}$$

The inflow mass fractions Y_{j0} correspond to a methane-air mixture with an equivalence ratio equal to 0.8. The boundary conditions for the walls labeled 'cooled' are given by

$$T = 333K, \quad v = u = \frac{\partial Y_j}{\partial \boldsymbol{n}} = 0, \quad j = 1, \cdots, N_s - 1. \tag{7.2}$$

The symmetry with respect to the center of the domain is described by

$$\frac{\partial T}{\partial x} = \frac{\partial v}{\partial x} = u = \frac{\partial Y_j}{\partial x} = 0 \quad , \quad j = 1, \cdots, N_s - 1. \tag{7.3}$$

At the outflow boundary, finally, we impose

$$\frac{\partial T}{\partial y} = p = u = \frac{\partial Y_j}{\partial y} = 0 \quad , \quad j = 1, \cdots, N_s - 1. \tag{7.4}$$

The initial conditions are given by the steady state for a flame with initial velocity $v_0 = 90cm/s$. A time dependent solution is found when the inflow velocity is suddenly increased to $v_0 = 120cm/s$. The increased inflow raises the flame until it stabilizes at a new, larger stand-off distance. For the chemistry in the flame we use a one-step reaction mechanism which includes the species methane, oxygen, water vapor, carbon dioxide and nitrogen. We shall only present the results concerning the temperature T, the vertical velocity v and the pressure p. These quantities were chosen in order to have one variable from each of the vectors $\boldsymbol{\phi}$, $\boldsymbol{v}$ and $\boldsymbol{p}$ (cf. Section 3). In Figure 4, the initial and final temperature fields are compared with experimental data. The rather large difference which is found in the stand-off distance is mostly a result of the one-step reaction mechanism, which is a somewhat crude model.

Figure 5 gives an impression of the time evolution of the flame. The 2-norm (mean square norm) of the approximate temperature-time derivative, $\|\boldsymbol{T}_n - \boldsymbol{T}_{n-1}\|/\Delta t$, is plotted as a function of time. Similar plots are shown in Figure 6 and 7, for the velocity and for the pressure, respectively.

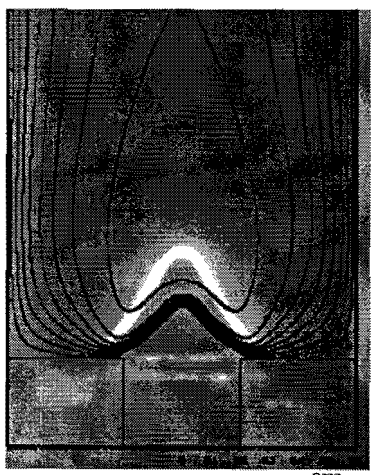

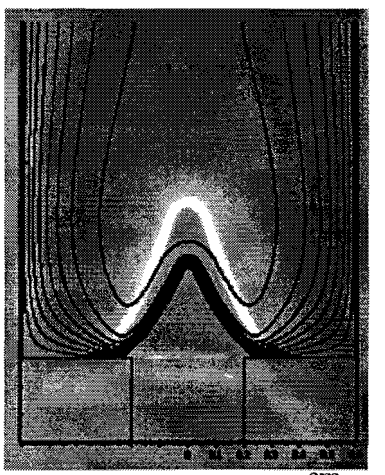

Figure 4: Isolines of calculated temperature, superimposed on photographs of experimental gas flames. Initial solution (left) and final solution(right).

The simulation was carried out three times: once on a coarse grid of 8100 points using the three-stage method and time steps $\Delta t \leq 10^{-4}s$, and twice on a finer grid of 31,500 points using both the two and three-stage methods, and time steps $\Delta t \leq 2.5 \times 10^{-5}s$. The continuity correction method (5.6a-d) was found to diverge. In Figures 5 and 6, a good agreement is found among the three methods. The pressure, however, appears to be much harder to predict. The three-stage method, however, appears to be more stable and produces a smoother graph.

8 Conclusion

In this paper, the causes have been identified for the computational difficulties encountered when doing combustion simulation using the Euler Backward time integration scheme, and the standard pressure correction scheme which we called the 'continuity correction method'. The analysis led to the formulation of two new pressure correction methods, which we called the two-stage and three-stage pressure correction schemes. The two-stage pressure correction scheme enforces the constraint imposed on the velocity field, while the three-stage scheme also enforces the pressure equation.

We may conclude, considering the numerical data and the fact that for complicated combustion problems the three-stage method is hardly more expensive than the two-stage method, that the three-stage method is superior to the two-stage method, and that the continuity correction method is to be rejected, on the basis of numerical data and Theorem 5.1.

Acknowledgement
The support of Gastec n.v. and EnergieNed, the Netherlands, is gratefully acknowledged.

References

[1] H. Bijl and P. Wesseling, *A method for the numerical solution of the almost incompressible Euler equations*, Report 96-37, Faculty of Technical Mathematics and Informatics, Delft University of Technology, Delft, 1996.

[2] M.Braack, *An adaptive finite element method for reactive-flow problems*, Ph.D. Thesis, Ruprecht-Karls University of Heidelberg, 1998.

[3] A.J. CHORIN, *The numerical solution of the Navier-Stokes equations for an incompressible fluid*, Bull. Am. Math. Soc. 73(6):928, 1967.

[4] P.M. GRESHO AND R.L. SANI, *Incompressible flow and the finite element method*, Wiley, Chichester, 1998.

[5] E. HAIRER AND G. WANNER, *Solving ordinary differential equations II, Stiff and differential algebraic problems*, Springer, Berlin, 1991.

[6] R.I. ISSA, *Solution of the implicitly discretized fluid flow equations by operator-splitting*, J. of Comput. Phys. 62, 40-65, 1985.

[7] R.J. KEE, F.M. RUPLEY AND J.A. MILLER, *The Chemkin thermodynamic data base*, SANDIA REPORT SAND87-8215, Sandia National Laboratories, Albuquerque, New Mexico 87185 and Livermore, California 94551.

[8] A. MAJDA AND K.G. LAMB, *Simplified equations for low Mach number combustion with strong heat release*, Dynamical issues in combustion theory, The IMA volumes in mathematics and its applications, volume 35, pp 167-211, Springer, 1991.

[9] S.V. PATANKAR, *Numerical heat transfer and fluid flow*, McGraw-Hill, New York, 1980.

[10] L.M.T. SOMERS, *The simulation of flat flames with detailed and reduced chemical models*, Ph. D. Thesis, Eindhoven University of Technology, 1994.

[11] R. TEMAM, *Analyse mathématique sur l'approximation des solutions des équations de Navier-Stokes*, C.R. Acad. Sci. Paris, Sér A, 262:219-221, 1966.

[12] J. WEICKERT, *Application of the theory of differential-algebraic equations to partial differential equations of fluid dynamics*, PhD thesis, TU Chemnitz-Zwickau ,1997.

[13] F.A. WILLIAMS, *Combustion Theory*, 2nd ed., Addison-Wesley, Redwood City, 1985.

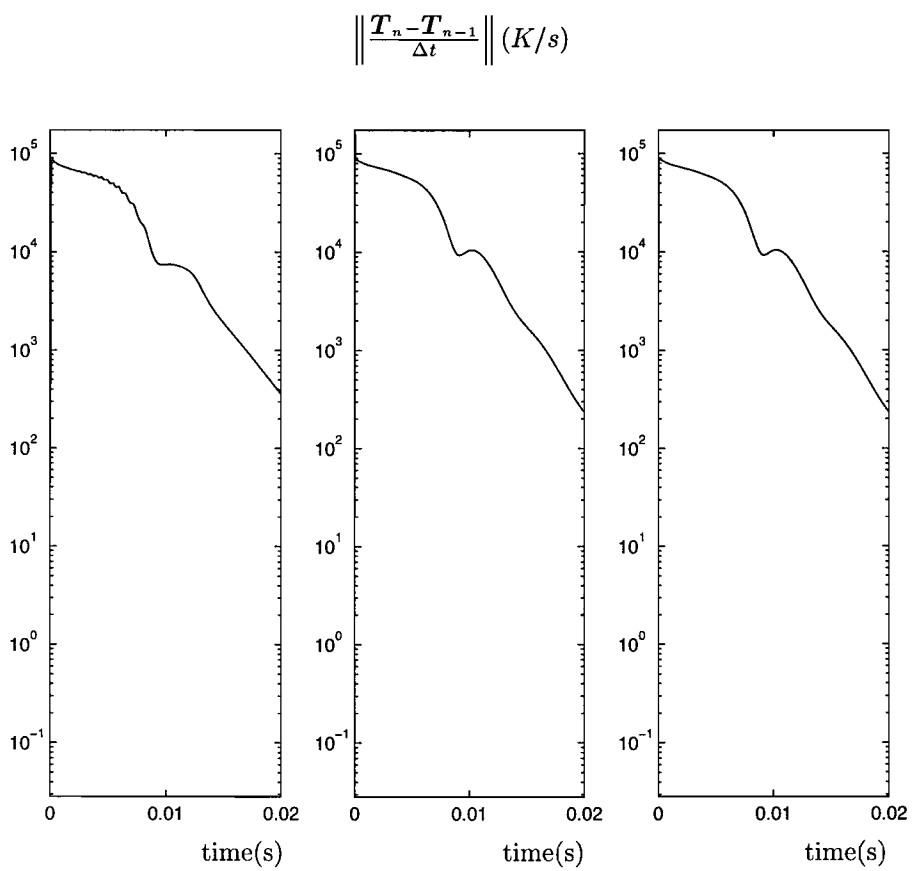

Figure 5: Predicted time evolution of the temperature-time derivative. Left: coarse grid, three-stage method. Middle: fine grid, two-stage method. Right: fine grid, three-stage method.

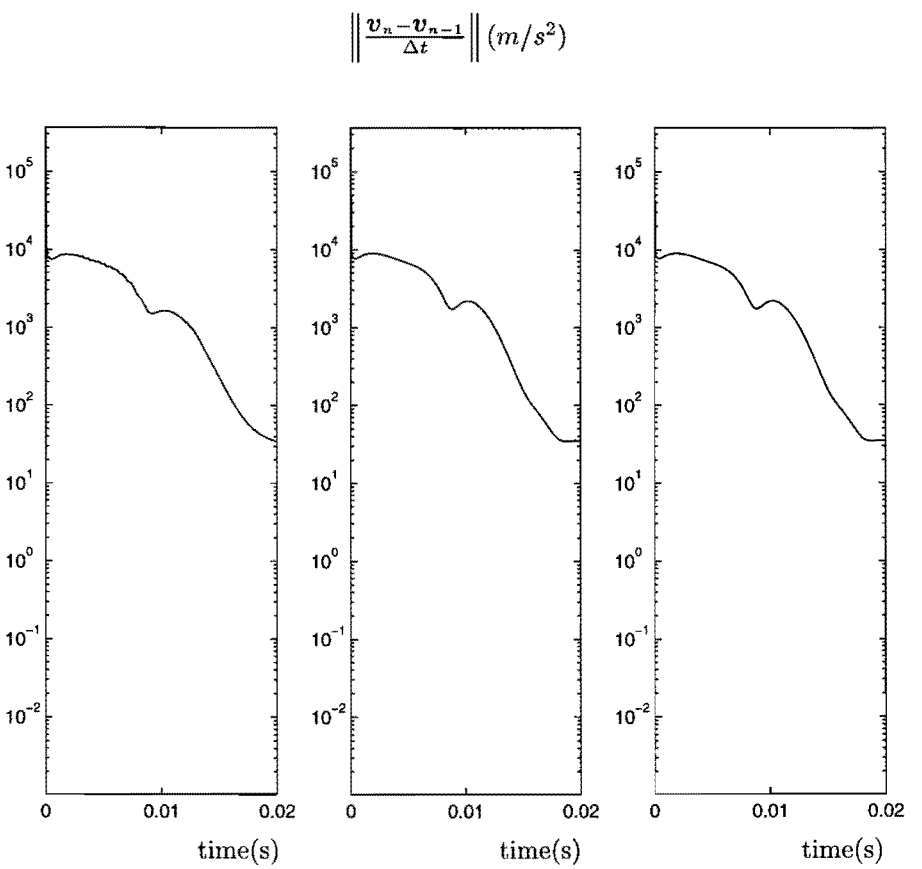

Figure 6: Predicted time evolution of the velocity-time derivative. Left: coarse grid, three-stage method. Middle: fine grid, two-stage method. Right: fine grid, three-stage method.

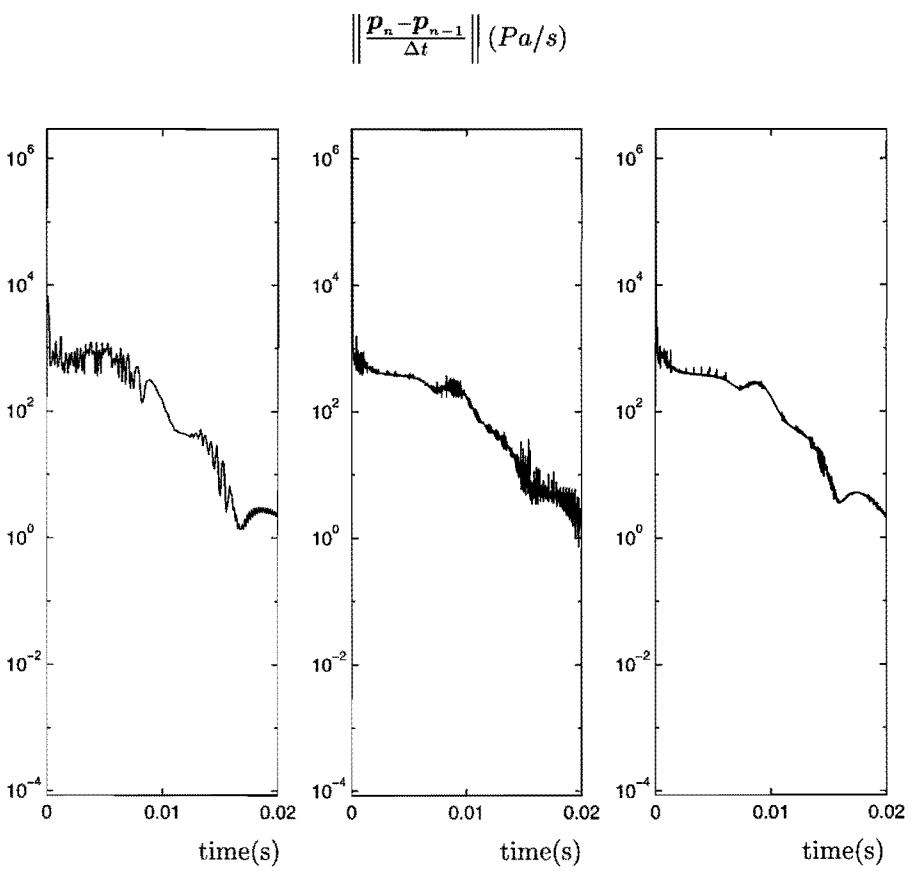

Figure 7: Predicted time evolution of the pressure-time derivative. Left: coarse grid, three-stage method. Middle: fine grid, two-stage method. Right: fine grid, three-stage method.